J Mol Model (2010) 16:1853–1865
DOI 10.1007/s00894-010-0681-0

ORIGINAL PAPER

Effect of piratoxin II and acutohaemolysin phospholipase (PLA2) proteins on myristic fatty acid—An ONIOM and DFT study

Angamuthu Abiram · Ponmalai Kolandaivel

Received: 27 September 2009 / Accepted: 29 January 2010 / Published online: 12 March 2010

Abstract A theoretical investigation on the interaction of myristic fatty acid (M) with Acutohaemolysin and Piratoxin-II of PLA2 family is performed using two layered ONIOM (B3LYP/6-31G*: UFF) method. The results predict that though proteins show revulsion to incoming fatty acid, the interaction of the phenyl ring of Phenylalanine restricts the passage of M through the channel. To unveil the nature of interaction of M, quantum chemical studies are carried out on the palindromic tripeptides Alanine-Phenylalanine-Alanine (AFA) and Alanine-Valine-Alanine (AVA) present in Acutohaemolysin and Piratoxin-II at B3LYP/6-311G** level of theory. The mode of interaction of the fatty acid with protein is electrostatic, confirmed further through molecular electrostatic potential (MEP) maps. The AFA shows stronger interaction than AVA, validating the impact of mutation on catalytic activity. Further such strong interaction and hence the higher probability of prohibition for catalytic activity exists only when the fatty acid interacts at the center of phenyl ring than at its edges. The preferred secondary structural configuration and conformational properties of AVA and AFA also validate the strong interaction of fatty acid with Phenylalanine. In general, this theoretical investigation shows that the loss of catalytic activity would take place only when fatty acid interacts at the center of phenyl ring.

Keywords Conformation · Density functional theory · Molecular electrostatic potential · Oniom · Phospholipase · Snake venom

A. Abiram · P. Kolandaivel (✉)
Department of Physics, Bharathiar University,
Coimbatore 641 046, India
e-mail: ponkvel@hotmail.com

Introduction

Snake venoms are complex mixtures of proteins, including phospholipases A2 (PLA2), myotoxins, proteolytic enzymes, neurotoxins, cytotoxins, cardiotoxins and others. Among these, the most potent toxic protein is the PLA2 which is wide spread in nature from viruses to human as extracellular and intracellular enzymes [1, 2]. PLA2 of snake venoms in addition to digestion, exhibit many pharmacological effects by disturbing the normal physiological process of victims [3–6]. Further they induce a complete failure of neuromuscular transmission leading to death of the prey due to paralysis of respiratory muscles [7]. Other effects of PLA2s include myonecrosis, neurotoxicity, cardiotoxicity, hemolytic, hemorrhagic, hypotensive, anticoagulant, platelet aggregation inhibition and edemainducing activities [2, 8]. However, the primary function of PLA2 is to hydrolyze the sn-2 ester bond of glycerophospholipids, to produce free fatty acids and lysophospholipids [9]. Scientists have proposed several models [3, 10–12] to explain the catalytic and pharmacological activities of PLA2s. Even though the catalytic activity of PLA2 contributes to various pharmacological effects, it is not a prerequisite [13–17].

Acutohaemolysin, a Lys49 PLA2, isolated from the venom of *Agkistrodon acutus,* unlike others lack both catalytic and hemolytic activity [18]. Comparison of the primary structure of Acutohaemolysin with other Lys49 PLA2 structures however shows a high degree of homology. The crystal structure determination of this protein to investigate the structural basis of its inactivity indicated that specific substitutions at residue 102 may be responsible for this catalytic loss. By sequence alignment, Phe102 was detected as a unique residue which exists only in Acutohaemolysin, whereas other Lys49 PLA2s possess

a short side-chain residue (*i.e.*, Valine) at this site. Comparison of the local conformation near the catalytic triad of Acutohaemolysin with that of piratoxin II, a catalytically active Lys49 PLA2 in complex with myristic fatty acid [19], apparently showed that the benzene ring of Phe102 interferes with the binding of potential substrates. Due to this, the docking of a similar (a 14-carbon fatty acid molecule) or larger fatty acid molecule into the hydrophobic channel of Acutohaemolysin seems to be prohibited. Though reason for the failure of catalytic activity is renowned, the atomistic behavior of myristic fatty acid with Piratoxin II and Acutohaemolysin is still unexplored. The nature of interaction of the fatty acid with Valine residue of Piratoxin II and mutated active site Phenylalanine residue of Acutohaemolysin is also unknown. Furthermore, these residues are found to be present in the helical region of respective proteins, and it is thus significant to explore and compare their conformational flexibility in the isolated form and in complex with myristic fatty acid, which will especially provide a clear picture on the loss of catalytic activity in Acutohaemolysin.

On the other hand, hybrid techniques such as QM/MM and ONIOM that combine two or more computational methods in one calculation are very successful in exploring the chemistry of large biological systems [20–22]. The geometry optimization of macromolecules are relatively faster in these multilevel hybrid methods as the active site regions are treated at a quantum mechanical (QM) level and the remaining regions treated by an inexpensive method such as molecular mechanics (MM). Thus in the present study, we have used ONIOM model to investigate the interaction of myristic fatty acid (M) with Acutohaemolysin and Piratoxin II of the PLA2 family. Also, we have applied quantum chemical calculation to gain more insight on the behavior of fatty acid with the active site Phenylalanine residue (Phe 102) of Acutohaemolysin protein. For this we have considered the palindromic moiety Alanine-Phenylalanine-Alanine (AFA) present in Acutohaemolysin for our analysis. In order to understand why the interaction of myristic fatty acid (M) with Phenylalanine residue forbids the catalytic activity of Acutohaemolysin protein, we have also compared AFA with its counterpart Alanine-Valine-Alanine (AVA) present in Piratoxin II protein. The preferred secondary structural configuration and conformational properties of AFA and AVA tripeptides both in the presence and absence of myristic fatty acid were studied. This theoretical investigation may aid experimentalists to search further for the toxic/pharmacological effects of PLA2 proteins.

System set-up and computational details

The goal of an efficient geometry optimization scheme is to find the optimized geometry with the least expenditure of computational effort which is feasible through hybrid ONIOM method. We have used in the study the two layered ONIOM (MO: MM) method with dft as *high level* MO region containing Becke's three-parameter non-local hybrid exchange functional with the non-local correlation functional of Lee, Yang, Parr named as B3LYP [23, 24] in concert with 6-31G* basis set [24] and the universal force field (UFF) as the *low level* MM region. Initially, the proteins Acutohaemolysin and Piratoxin II coded as 1MC2 and 1QLL respectively in the protein data bank (pdb) were extracted. As already known [18] the primary structure of all Lys49 PLA2 proteins show analogy having seven helices and two *beta* sheets but vary only by the mutation of few residues. On the other hand the earlier study [18] has suggested that the stacking of fatty acid in Acutohaemolysin may be due to its interaction with mutated Phenylalanine (Phe102) residue (Valine in the case of Piratoxin II) which is found to be present in the helical region. Thus for the ONIOM calculation, we have taken the particular helix (Gln 089—Asn 109, shown in Fig. 1 containing the Phe 102 from Acutohaemolysin. In this structure we have treated the fatty acid and Phenylalanine (Phe102) along with its neighboring residues Ala 101 and Ala 103 as *high level* regions (see Fig. 1) and the remaining protein environment as *low level*. Similarly in the case of Piratoxin II, same helix, Asn 79—Asn 99 is considered wherein the fatty acid and Valine (Val 92) along with its neighboring residues Ala 91 and Ala 93 were treated as *high level* regions and the remaining protein as *low level*. The complexes were constructed by placing the myristic fatty acid at different positions near Phe 102 and Val 92 and are optimized using the ONIOM (MO: MM) method as explained above. Even though we have considered only the helix containing active site residue (Phe102/ Val 92), the fatty acid is expected to interact also with other regions of the protein. However, since quantum mechanical calculations cannot be performed for the whole protein even with the help of super computers and owing to constrain that we had in the computational requirements we restricted the system to a single helix. On the other hand we expect those effects will have less influence on the interaction between the active site and fatty acid. However, a complete molecular dynamics study on the behavior of the fatty acid with the full protein (containing the seven helices and two *beta* sheets) is still needed, to gain more information about the protein-fatty acid interaction and is to be done in the near future.

To obtain an in-depth knowledge on the interaction of fatty acid with the active sites of the proteins, the binding energies for the high level regions were calculated at B3LYP/6-31G* level of theory using Eq. 1,

$$\Delta E = (E_{AB} - (E_A + E_B)). \quad (1)$$

In Eq. 1, E_{AB} represents the total energy of the *high level* regions calculated from the ONIOM (MO: MM)

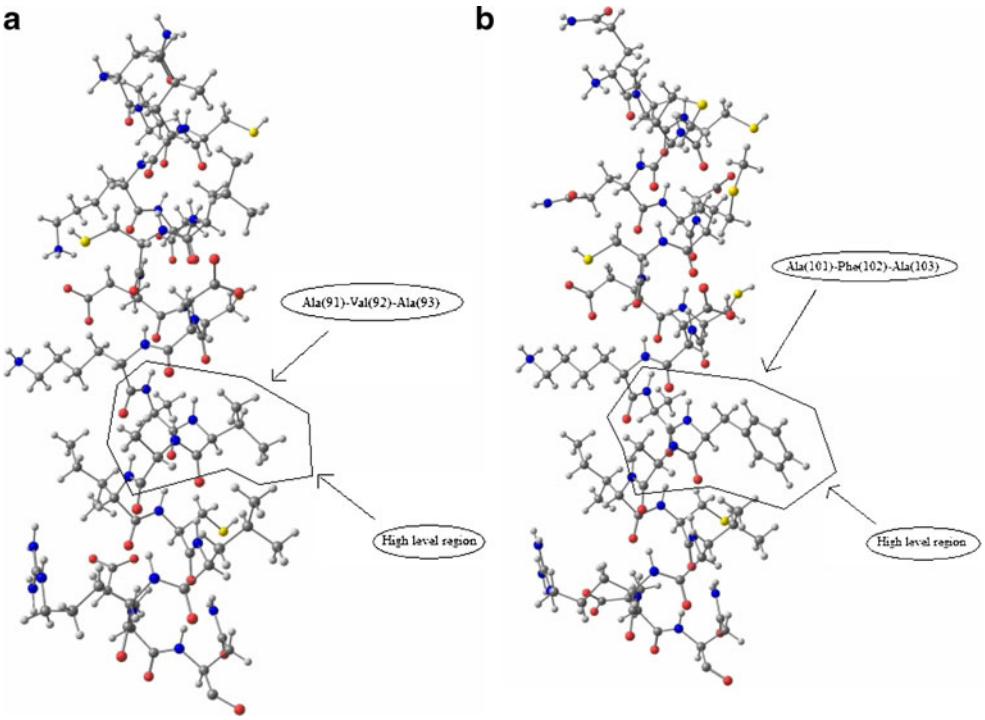

Fig. 1 **a** Helix (Gln 089—Asn 109) extracted from the protein Acutohaemolysin for ONIOM calculation wherein the marked region constituting Ala 101, Phe 102 and Ala 103 represent the high level region while the other are at low level and **b** Helix (Asn 79—Asn 99) extracted from the protein Piratoxin II for ONIOM calculation wherein the marked region constituting Ala 91, Val 92 and Ala 93 represent the high level region while the other are at low level

method. E_A represents the optimized energy of myristic fatty acid and E_B the optimized energy of AFA/AVA. To know further about the atomistic behavior prevailing between the fatty acid and the active site residue of the protein, quantum chemical calculations at B3LYP/6-311G** level of theory was also performed. For this we have considered the palindromic tripeptides AFA and AVA from the respective proteins and they were optimized. The optimized tripeptides were then made to interact with myristic acid (M), and a complete optimization of the formed AFA-M and AVA-M complexes were also performed at B3LYP/6-311G** level of theory. Harmonic vibrational frequency analyses suggested that all the optimized structures belong to minima in the respective potential energy surfaces.

The Ramachandran map [25] is a well known tool to visualize dihedral angles φ against ψ and thereby to understand the minimum energy conformers (conformational minima) of amino acid residues in peptides and proteins. Thus to find the possible minimum energy conformers of AFA and AVA tripeptides in the presence and absence of myristic fatty acid, Ramachandran plot is employed. We have performed the potential energy surface (PES) scan for the main chain dihedral angles φ and ψ of Phenylalanine and Valine residues in AFA and AVA with an incremental step size of 50°. Further, in order to understand the reliability of complexes and the affinity of fatty acid on peptides in actual conditions, solvent reaction field calculations were also performed. Experimentally, Acutohaemolysin is purified and crystallized using isopropanol as the primary solvent [18]. Due to lack of this solvent, single point solvent reaction field calculations at B3LYP/6-311G** level of theory were performed in ethanol solvent for the *in vacuo* optimized geometries. The polarizable continuum method (PCM) developed by Tomasi and other co-workers [26–29] was used to calculate the free energy of solvation (ΔG) of isolated AFA and AVA, and their fatty acid complexes AFA-M and AVA-M.

The molecular interactive behavior prevailing between the peptide and fatty acid is further explored by the molecular electrostatic potential (MEP), a tool that explains the approach of chemical species near a molecule [30, 31]. The electrostatic interaction between a molecule and a test charge of magnitude 'e' (that is a proton) placed at a point r is well represented by the molecular electrostatic potential V(r) using Eq. 2,

$$V(r) = \sum_A \frac{Z_A}{|R_A - r|} - \int \frac{\rho(r')}{|r - r'|} dr', \qquad (2)$$

where Z_A is the charge on nucleus A located at R_A, that is considered to be a point charge and the second term arises from the electron density, ρ(r′), of the molecule that can be obtained computationally [32] or experimentally [33]. The molecular electrostatic potential at each atom of the structures has been obtained as a standard output from Gaussian 03 program package [34] at B3LYP/6-311G** level of theory. The graphical program gOpenMol [35] has been utilized to plot the data of molecular electrostatic potential.

Results and discussion

ONIOM energy and geometry

As already discussed in the computational part, complexes with a helix (containing 20 amino acids) and myristic fatty acid are considered for the ONIOM study. Since it is a system of larger size many local minima for the complex is thus expected. Initially, many complexes were constructed by placing the myristic fatty acid at the different positions of the active site (Phe102/ Val 92) and the geometry ONIOM optimization was performed. However, for most of the conformers the convergence criterion was not met and by changing the position of the fatty acid again and again, finally, we got these complexes optimized. Even though there may be other local minima we expect these to be one of the local minimum structures.

The initial structure of the complex, helix of protein Piratoxin II with myristic fatty acid is hereafter referred as PII-M and is shown in Fig. 2. The interaction of the fatty acid seems to have good impact on the protein as it has undergone distortion during optimization clearly seen from the optimized PII-M structure (see Fig. 3). The fatty acid initially placed near the protein, during optimization moves well inside. But is there an interaction of the fatty acid with the Val 92 residue or any other residues nearby? If we take a closer view of the optimized PII-M structure, it is very clear that while the fatty acid moves closer toward the protein, the residues nearby show revulsion and moves away from M. This hatred of the residues has led to the distortion of the structure during optimization. It is now significant to see whether there is a considerable interaction between M and Val 92 or nearby residues. The interaction energy calculated for the *high level regions*, *i.e.*, the ΔE between M and AVA is found to be only −7.09 kcal mol^{-1} and this seems to have no significant impact on the protein structure. Thus Val 92 residue plays no role in obstructing the fatty acid and allows it to pass though the hydrophobic channel.

However in protein Acutohaemolysin, where there is a mutation of Valine by Phenylalanine residue, the same effect is not expected [18]. The interaction of phenyl ring with the fatty acid prohibits the passage of the latter into the channel which in turn leads to the stacking of similar fatty acids. The earlier study however has not confirmed the actual position at which the incoming fatty acid interacts with the protein. Thus the complexes, helix of protein Acutohaemolysin with myristic fatty acid hereafter referred as A-M are constructed by placing the myristic fatty acid at two different positions of the phenyl ring of Phe102 residue. First the myristic fatty acid is placed at the center of the phenyl ring and later the same at its edges (see Fig. 2 b and c). In both the complexes the carboxylic group of the fatty acid is made to face the phenyl ring and these are

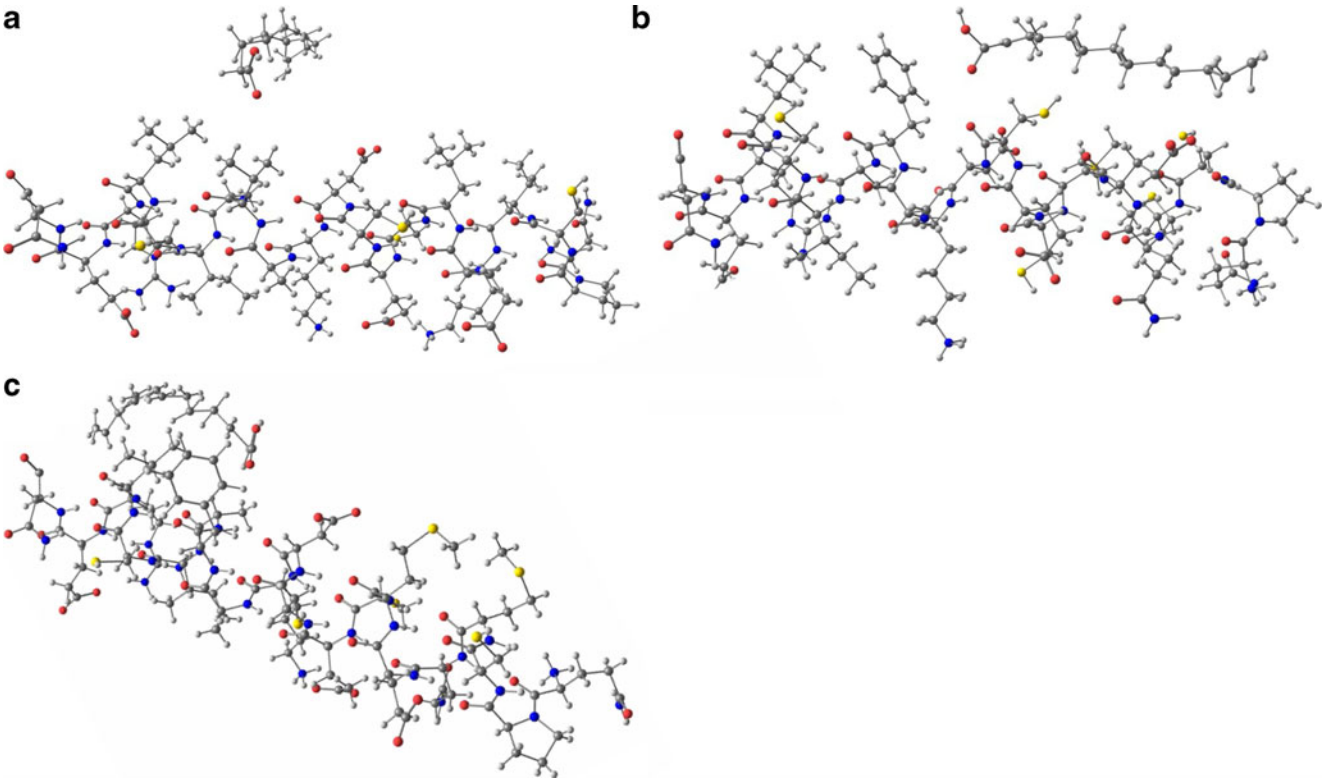

Fig. 2 Initially constructed complexes for ONIOM (B3LYP/6-31G*: UFF) calculation **a** PII-M, **b** A-M(C) and **c** A-M(E)

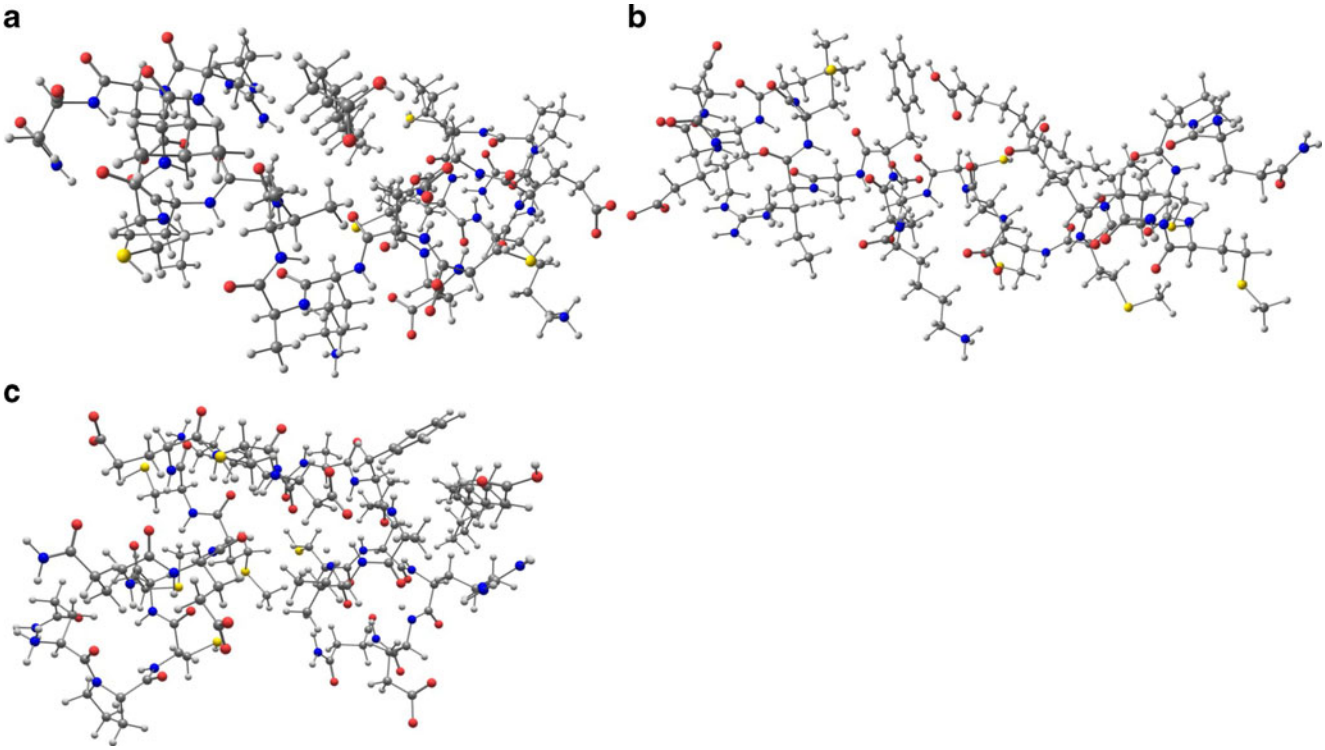

Fig. 3 ONIOM (B3LYP/6-31G*: UFF) optimized complexes **a** PII-M, **b** A-M(C) and **c** A-M(E)

hereafter referred as A-M(C) and A-M(E). The initially constructed A-M(C) and A-M(E) complexes are shown in Fig. 2 and the ONIOM optimized structures are shown in Fig. 3. Both the complexes show larger distortion of the helix, clearly seen from the optimized structures.

In the case of A-M(C) complex, the carboxylic group of M stays close to the phenyl ring indicating that a sharing of the π clouds of the aromatic ring is taking place with its hydroxyl hydrogen. Also, throughout the optimization the phenyl ring does not show much deviation from its position even though other residues have moved away from the incoming fatty acid. The calculated distances between the carboxylic group of M and the phenyl ring is around 2.73 Å. Though the interaction of M with Acutohaemolysin seems to be weak, the presence of Phe102 is expected to increase the interaction in A-M(C) compared to the PII-M complex. The calculated interaction energy for the *high level regions*, *i.e.*, ΔE between M and AFA confirms this prediction as it is found to be −28.46 kcal mol^{-1}, which is −21.37 kcal mol^{-1} larger in energy than the PII-M complex. Thus it is now clear that the mutation of Valine residue by Phenylalanine leads to the stacking of fatty acids [18], but the question at what position actually the fatty acid interacts with the phenyl ring is still unanswered. For this let us see what happens when the fatty acid interacts at the edge of the phenyl ring.

During the optimization of the initially constructed A-M(E) complex (see Fig. 2c) the fatty acid undergoes larger distortion and moves well within the secondary structure. Finally M reaches a comfortable position as shown in Fig. 3 where the complex finds its local minima. Here, it is not the carboxylic group but it is the long chain methyl group of M that interacts with the phenyl ring. The comparison of the optimized energies of the *high level region* between A-M(C) and A-M(E) predict that the former is around 1.25 kcal mol^{-1} less in energy than the A-M(E) complex. However, the calculated interaction energy of the *high level region* of A-M(E) complex is found to be −28.25 kcal mol^{-1} which is almost similar to that of the A-M(C) complex. Thus by comparing the energy minima of the two complexes we can say that the interaction of the carboxylic group of fatty acid with the aromatic ring of the Phenylalanine, *i.e.*, A-M(C) complex is the most suitable one to prevail. In order to obtain more detailed information on the fatty acid interaction with the active site residues, we decided to go for a complete quantum chemical calculation of the *high level regions,* and it is explained below.

Quantum chemical study

For quantum chemical study, the *high level regions* considered for ONIOM calculations namely AVA of Piratoxin II and AFA of Acutohaemolysin are taken for the interaction with fatty acid (M). M is made to interact with the tripeptide AVA at the same position as in the

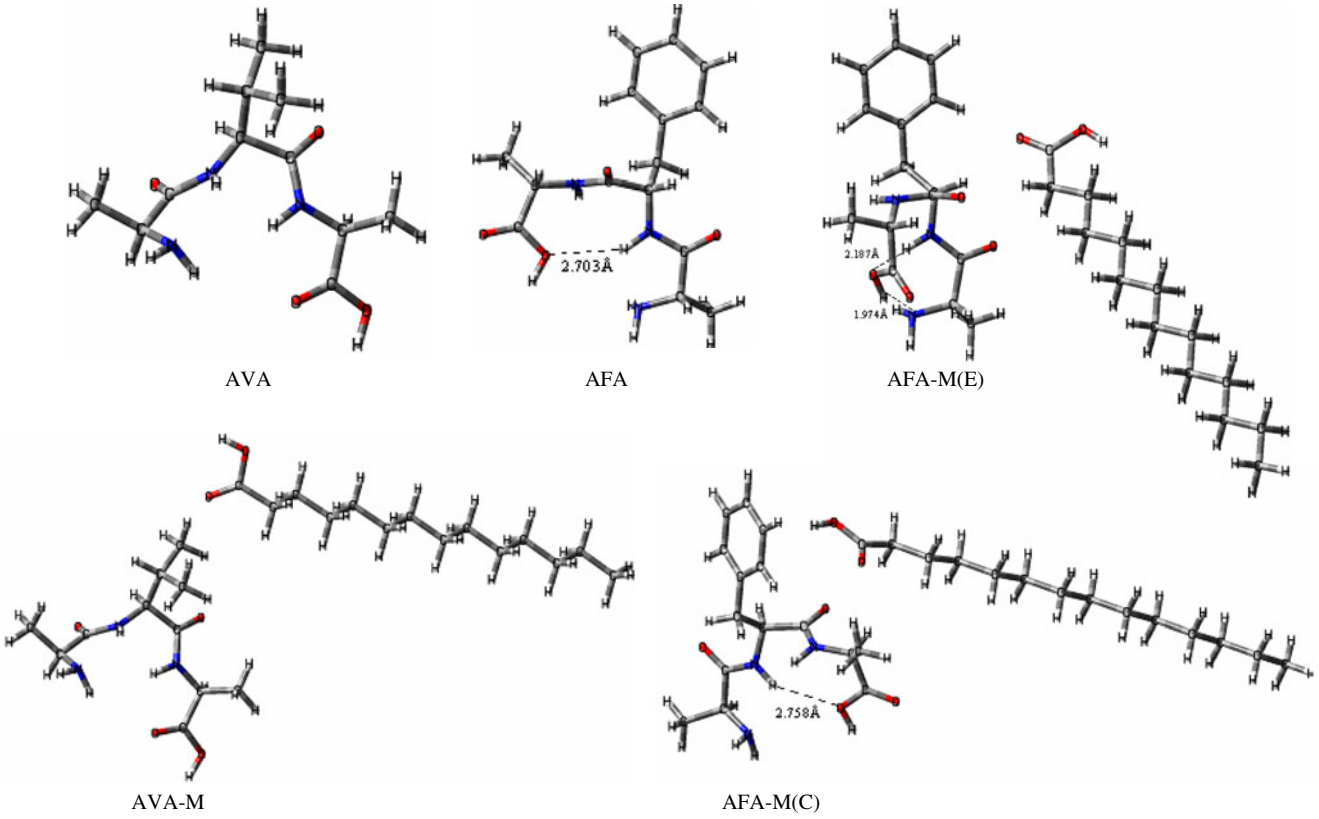

Fig. 4 Three dimension structure of AVA, APA and its complexes optimized at B3LYP/6-311G** level of theory

ONIOM method and the complex formed is hereafter denoted as AVA-M. In the case of Acutohaemolysin, the same positions taken for ONIOM method a) myristic fatty acid placed at the centerre of the phenyl ring (AFA-M(C)) and b) the same placed at its edges (AFA-M(E)) are considered. We also tried optimizing the complex where the long chain methyl group of the fatty acid interacts with the phenyl ring of Phenylalanine, *i.e.*, by keeping the fatty acid in the same position as in the ONIOM optimized A-M(E) complex. However, the convergence was not met and the structure fails to reach its local minima. All the above complexes were optimized at B3LYP/6-311G** level of theory and they are shown in Fig. 4.

Energy and geometry

The energies of the isolated structures of AVA and AFA palindromic tripeptides and their fatty acid interacted (AVA-M and AFA-M(C) and AFA-M(E)) complexes optimized at B3LYP/6-311G** level of theory are listed in Table 1. The optimized energy at B3LYP/6-311G** level of theory of AVA-M is found to be −1598.34 hartrees and that of AFA-M (C) and AFA-M(E) complexes are −1750.794 and −1750.781 hartrees respectively. Thus the optimized AFA-M(E) complex is higher in energy than AFA-M(C) complex with a barrier height of 8.16 kcal mol^{-1}, indicating that the AFA-M(C) complex is the most stable structure. This further shows that the myristic fatty acid has a maximum chance of interacting at the center of the aromatic ring of Phenylalanine residue than at the edges. Subsequently, in order to infer the stability of the complexes, single point solvation calculations in ethanol solvent were performed at B3LYP/6-311G** level of theory and are listed in Table 1. The negative ΔG values of all the structures clearly depict their reliability in actual conditions. The larger negative values of ΔG for AVA-M and AFA-M(C) complexes of the order approximately −2.5 kcal mol^{-1} than that of the AFA-M(E) complex might be due to the interaction of unprotected hydrogen atoms of

Table 1 Interaction energies ΔE (in kcal mol^{-1}), and solvation free energy ΔG (in kcal mol^{-1}) of the complexes optimized at B3LYP/6-311G** level of theory (A) and single point calculations at B3LYP/6-311++G** (B), MP2/6-31G* (C) and HF/6-311G** (D) levels of theory

Structures	ΔE				ΔG
	A	B	C	D	
AVA-M	−1.95	−0.91	−3.14	−1.32	−6.83
AFA-M(C)	−6.97	−4.96	−12.55	−5.90	−6.70
AFA-M(E)	1.19	4.14	−1.88	7.53	−4.33

Table 2 Main chain dihedral angles (units of degrees) of isolated and fatty acid interacted tripeptides optimized at B3LYP/6-311G** level of theory

Structures	Torsional angles					
	ψ_{i-1}	ω_{i-1}	ϕ_i	ψ_i	ω_i	ϕ_{i+1}
AVA	−16.11	−175.78	−107.97	−4.05	173.29	−157.24
AVA-M	−17.22	−176.62	−102.26	−8.16	172.85	−156.34
AFA	14.68	171.11	−156.00	−66.07	167.06	−100.91
AFA-M(C)	14.34	171.02	−155.42	−69.50	169.11	−94.44

solvent with the solute resulting in enthalpy contribution to the free energy of solvation [36].

To know how far the interaction is between the fatty acid and the tripeptides, the interaction energy is calculated for the optimized complexes at B3LYP/6-311G** level of theory and are listed in Table 1. It is clear from the table that the interaction energy of AFA-M(C) complex is more compared to the other two complexes. In order to compare the obtained interaction energy, single point interaction energy calculation was also performed at B3LYP/6-311++G**//B3LYP/6-311G**, MP2/6-31G*//B3LYP/6-311G** and HF/6-311G**//B3LYP/6-311G** levels of theory and are tabulated in Table 1. Even though the calculated interaction energies vary from one another (which may be due to the single point calculations), all of them predict AFA-M(C) complex to have the maximum interaction. This further substantiates that the myristic fatty acid will have a profound affinity to interact at the center of the aromatic ring of the Phenylalanine residue.

The main chain torsional angles of the isolated AVA and AFA palindromic tripeptides and their fatty acid interacted AVA-M and AFA-M(C) complexes are listed in Table 2. In AVA-M complex, the incoming fatty acid distorts the main chain dihedral angles φ and ψ of the intermediate Valine residue by 5° approximately. The carboxylic group of the fatty acid has no effect on the torsional angles of AVA tripeptide, which is further confirmed by the remaining main chain dihedral angles. This shows that the influence of Valine residue on the incoming fatty acid is negligible and hence tends to keep its neighboring residues rigid and inflexible. This rigidity of the structure and its revulsion to interact with the fatty acid aids the latter to pass through the channel and favor for catalytic and hemolytic activities [18]. The φ and ψ dihedral angles of the Phenylalanine in isolated AFA are found to be −156.0° and −66.07°, whereas after interaction with myristic fatty acid φ and ψ angles vary slightly to −155.42° and −69.50° respectively, maintaining rigidity in the structure. However, in AFA-M(C) complex, the fatty acid is found to align itself in such a way that its carboxyl group faces the six membered aromatic ring of Phenylalanine residue. Hence, as from the explanation of Qun Liu et. al. [18] the presence of the aromatic ring of Phe102 is expected to interfere with the fatty acid.

Thus it is also necessary to look into the conformation of six-membered phenyl ring of Phenylalanine to check any variations are caused by the fatty acid. The endocyclic torsion angles (see Fig. 5b) of the phenyl ring present in the AFA structure before and after interaction of the fatty acid are listed in Table 3. As expected, the six membered phenyl ring has a causal role on the incoming fatty acid. The significant variation of endocyclic torsion angles clearly predicts considerable interaction between the π cloud of benzene ring and carboxylic group of fatty acid. Due to rigidity of the structure the interaction may be weak, yet that is enough to hamper the fatty acid to pass through the channel for catalysis. These results coincide well with the early experimental study [18] and our ONIOM results confirming the interaction of fatty acid with the phenyl ring of Phenylalanine residue in Acutohaemolysin protein.

Hence, we can confirm that the mutation of Phenylalanine for Valine residue prohibits the entry of fatty acid inside the channel leading to the loss of catalytic activity. Moreover, this is possible only when the carboxylic group

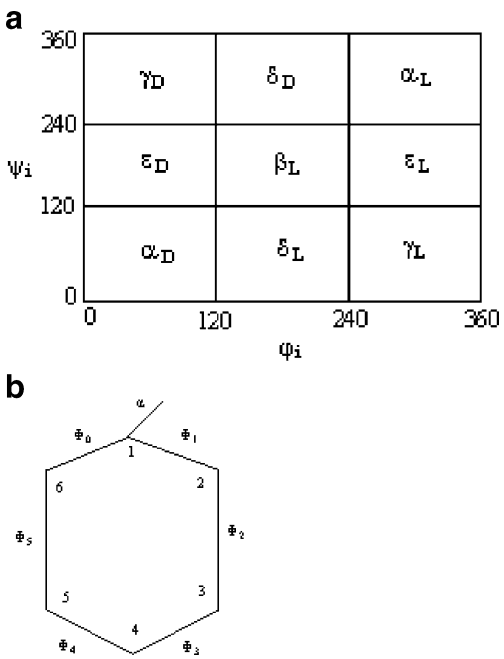

Fig. 5 **a** Standard backbone conformation regions [40] for amino acid residues in one dimension **b** Torsion angle numbering in the six-membered rings

Table 3 Endocyclic torsional angles (units of degrees) of isolated and fatty acid interacted tripeptide optimized at B3LYP/6-311G** level of theory

Structures	Endocyclic torsional angles					
	Φ_0	Φ_1	Φ_2	Φ_3	Φ_4	Φ_5
AFA	−0.125	0.156	−0.018	−0.153	0.182	−0.043
AFA-M(C)	−0.380	0.009	0.326	−0.298	−0.066	0.405

of the fatty acid interacts at the center of the phenyl ring of Phenylalanine than at its edge.

Conformational analysis

The core objective of conformational energy calculations on peptides and proteins is to analyze and predict their three-dimensional structures, stability, and dynamic properties [37–39]. However, for the structures of peptides and proteins, their folding and motions are most often described using a simplified rigid model with fixed bond lengths and bond angles. In such a model, torsion angles (φ, ψ and ω) per amino acid residue are employed to describe the main chain folding. Since ω describes the rotation of the amide bond which is typically 180º (seldomly 0º), the knowledge of the first two angles is often sufficient. Here, since the palindromic tripeptides are helical structures, it is significant to identify their conformational changes in the presence and absence of myristic fatty acid by changing the main chain torsion angles (φ and ψ) of Valine and Phenylalanine

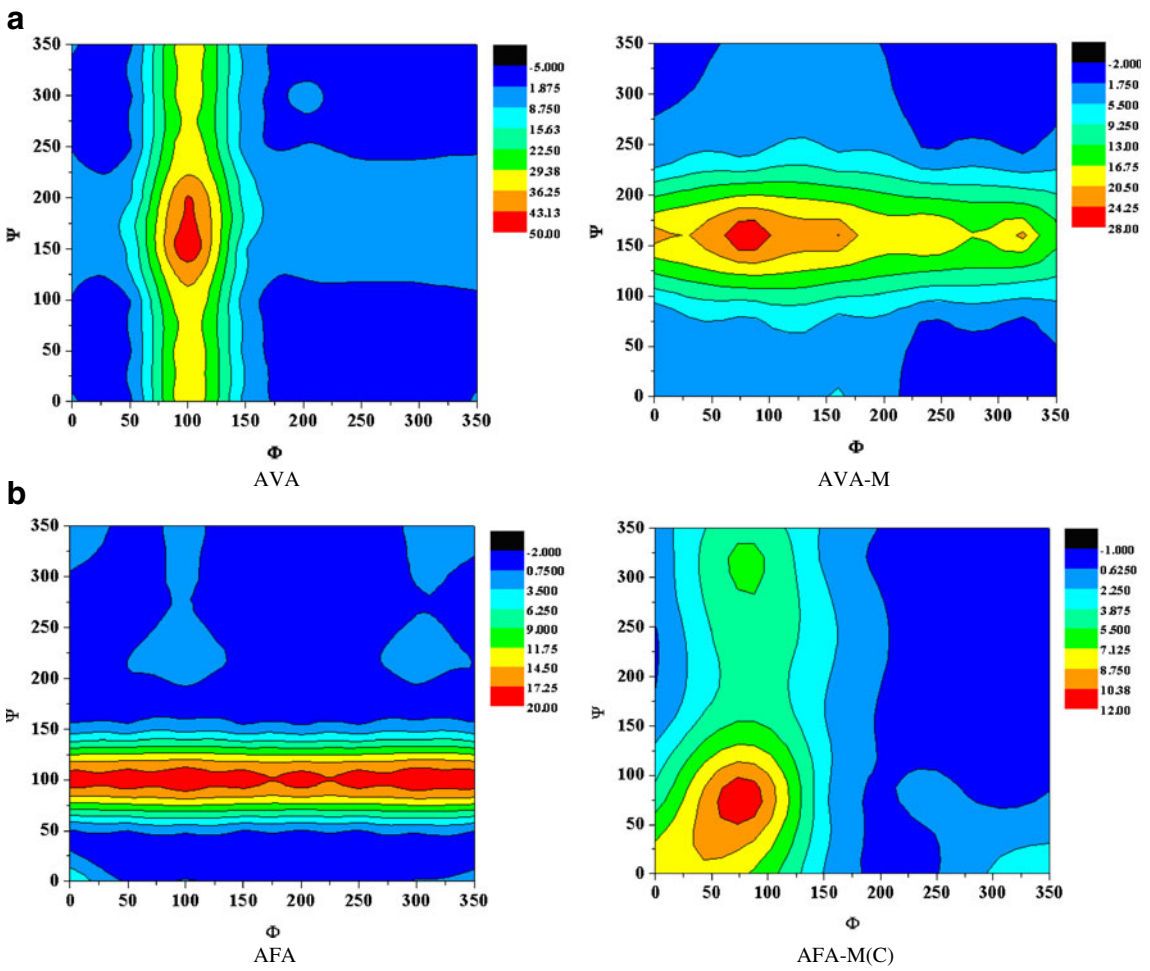

Fig. 6 The Ramachandran plot for all the structures calculated at B3LYP/6-311G** level of theory **a** corresponds to the complete 0º to 360º variation of φ and ψ torsion angles of the Valine residue in AVA and AVA-M and **b** corresponds to the complete 0º to 360º variation of φ and ψ torsion angles of the Phenylalanine residue in AFA and AFA-M. The φ and ψ torsion angles are in degrees and the color scheme represents the relative energies in hartrees

residues in the respective tripeptides. It is well known that, based on the φ and ψ torsion angles, the conformers of structure can be categorized to α_D, α_L, β_L, γ_D, γ_L, δ_D, δ_L, ε_D and ε_L regions using the standard backbone conformation [40] shown in Fig. 5a. The conformations of AVA and AFA in their isolated forms and in complex with fatty acid (M) obtained from PES scan are categorized by means of Ramachandran plot as shown in Fig. 6. We have carried out the PES scan of AVA and AFA by changing the main chain torsion angles φ and ψ of Valine and Phenylalanine residues from 0º to 360º with the incremental step size of 50º. However throughout this study the position of the myristic fatty acid (M) is never changed and it is at the same position as obtained from the geometry optimization of AVA-M and AFA-M(C) complexes. Figure 6 represents the complete PES of AVA and AFA tripeptides both in the presence and absence of myristic fatty acid. It shows the most and least possible conformers of AVA to be in γ_L, α_L, α_D, γ_D, δ_L and δ_D regions, and ε_D, ε_L and β_L regions respectively. The minimum energy conformers of AFA tripeptide are found to be present in almost all the regions, whereas its higher energy conformers prevail in the regions other than γ_D, δ_D and α_L. Thus, the plots in Fig. 6 show all the maximum and minimum energy regions of the AVA, AFA, AVA-M and AFA-M(C). In order to identify the lowest energy conformation, *i.e.*, the global minima, we have selected all possible low energy conformers obtained from PES and represented in Ramachandran plot of Fig. 7.

In AVA, while changing the φ and ψ torsion angles of Valine residue, the minimum energy conformers were found to exist in γ_L, α_L regions and also in α_D, γ_D, δ_L and δ_D regions (see Fig. 6) which is in good agreement with the literature data [41]. However, the most likely minimum energy conformers of AVA are found to be present in the γ_L and α_L regions which can be clearly identified from the Ramachandran plot for AVA shown in Fig. 7. Among these, the lowest energy conformer of AVA is found to prevail in the γ_L region with φ and ψ torsion angles of 250º and 0º

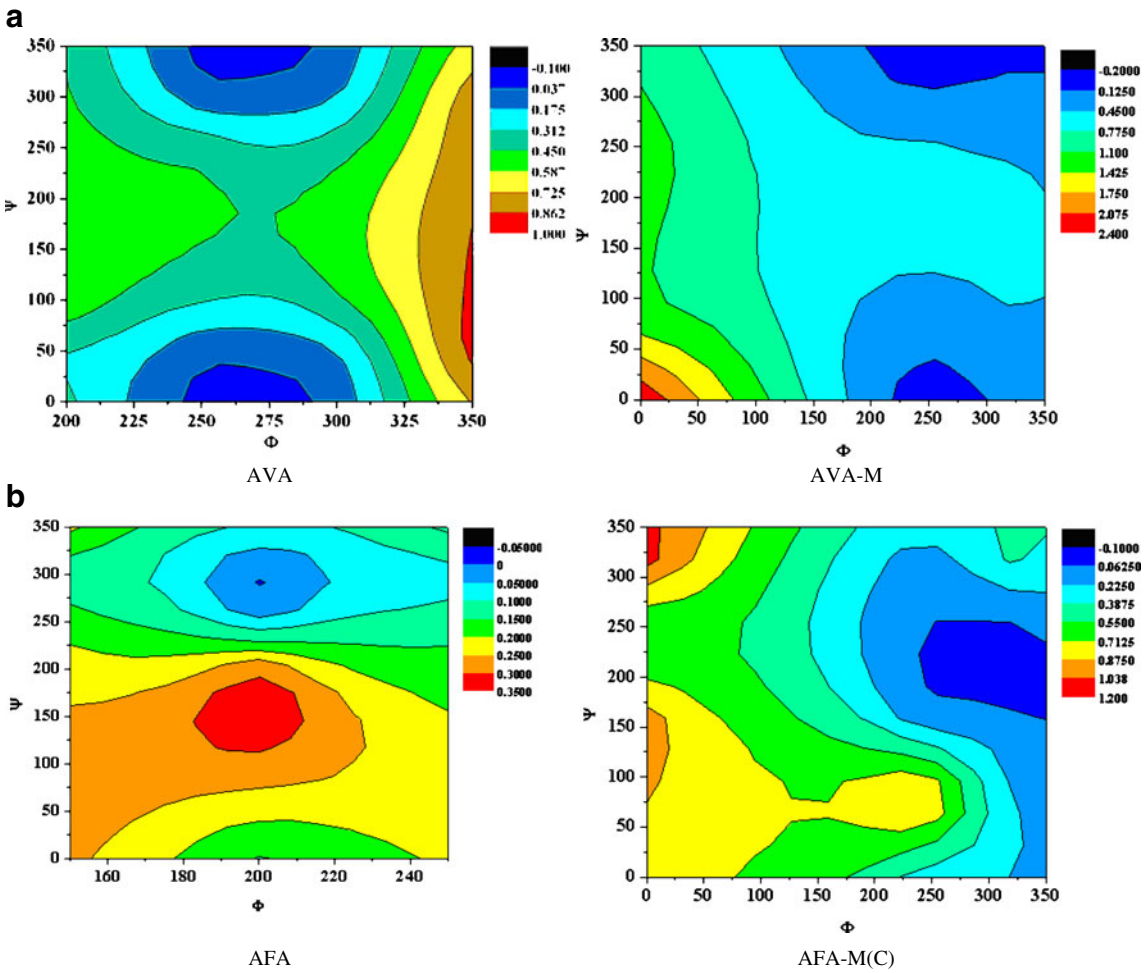

Fig. 7 The Ramachandran plot showing the global minimum of the structures: **a** AVA and AVA-M (for selected φ and ψ torsion angles of Valine residue) and **b** AFA and AFA-M (for selected φ and ψ torsion angles of Phenylalanine residue) calculated at B3LYP/6-311G** level of theory. The φ and ψ torsion angles are in degrees and the color scheme represents the relative energies in hartrees

respectively. After the interaction of fatty acid (*i.e.*, AVA-M), the PES of AVA shows that the minimum energy conformers do prevail in the γ_L, α_L, and γ_D regions (seen from Fig. 7). Similar to the isolated form, the lowest energy conformer of AVA in AVA-M still prevails in the γ_L region with φ and ψ torsion angles of Valine residue in 240º and 0º respectively.

The search for the minimum energy conformers of AFA palindromic tripeptide by varying the main chain φ and ψ torsion angles of Phenylalanine residue illustrates that the conformers exist in almost all the regions, which is easily identified from AFA Ramachandran plot in Fig. 6. This result is also found to be in analogy with the earlier study by Császár et al. [41]. The Ramachandran plot in Fig. 7 clearly pictures that the global minimum of AFA lies in the δ_D region with φ and ψ torsion angles of Phenylalanine residue at 200º and 300º respectively. In the case of AFA-M (C) complex, the fatty acid interaction on palindromic tripeptide seems to have an impact on the conformational subsistence of AFA. The minimum energy conformers of AFA after fatty acid interaction are found to restrict themselves to six possible regions namely α_L, ε_L, β_L, γ_L,

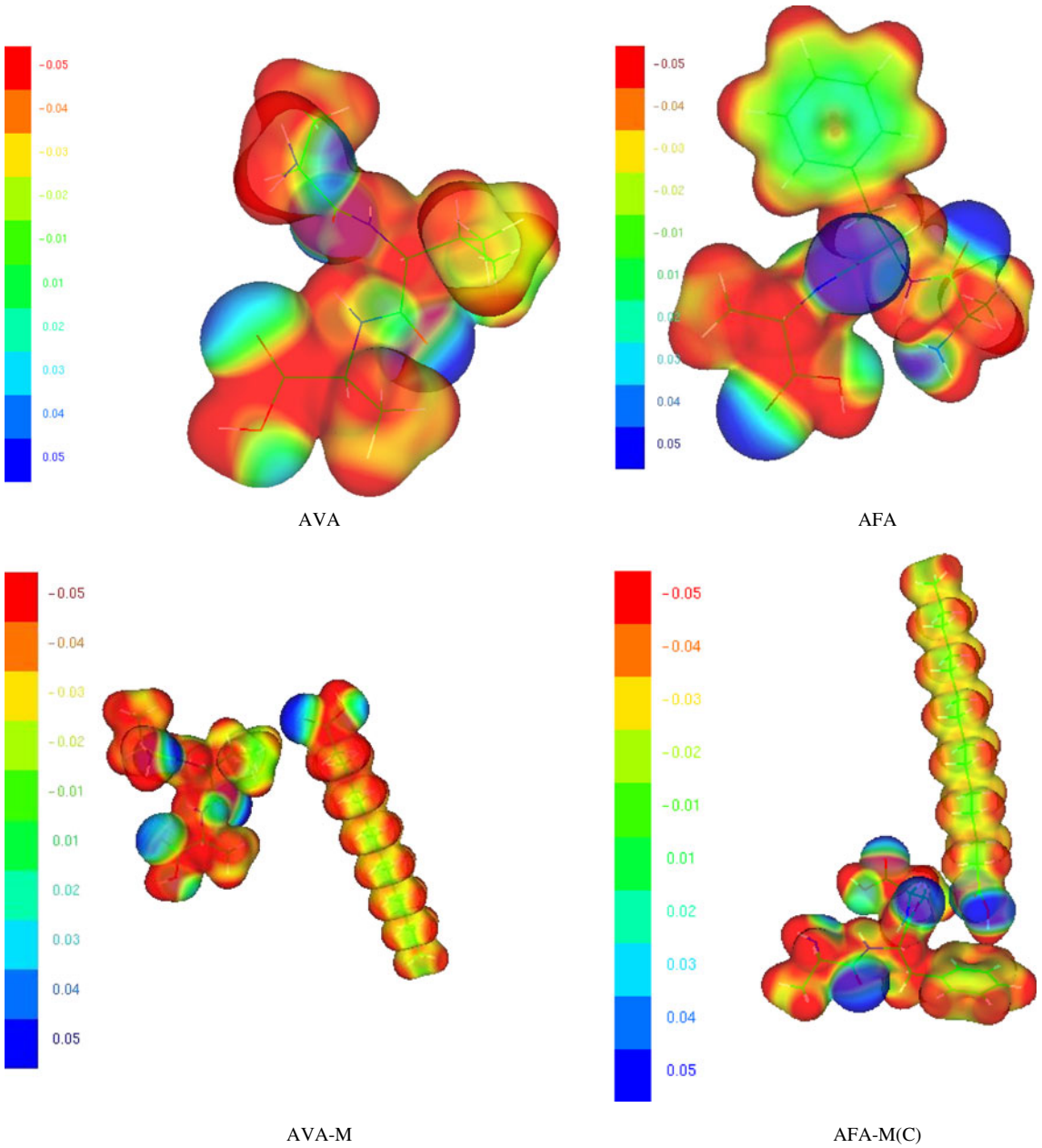

Fig. 8 The electrostatic potential of AVA, AFA and their fatty complexes mapped on the molecular isodensity surface (ρ=0.01a.u). Color scheme ranges from red (−0.05 a.u.) *via* green (zero) to blue (0.05a.u)

δ_D and δ_L. Among these regions, the maximum possibility for minimum energy conformers is found to be in the α_L and ε_L regions. Further, the AFA conformer with global minimum prevails in the α_L region with φ and ψ values of 320º and 240º respectively. Such variations in the minimum energy conformers of AFA from one region to another and the restriction of conformers to specific regions after the interaction of fatty acid are not found in AVA. In general, the PES of AVA and AFA palindromic tripeptides in the presence and absence of fatty acid clearly shows that the fatty acid M has more impact on the conformational existence of AFA than AVA tripeptide.

Molecular electrostatic potential (MEP)

The interaction of fatty acid with palindromic tripeptides is predominantly electrostatic in nature. The molecular electrostatic potential (MEP), a well-established tool for exploring molecular reactivities, intermolecular interactions and representing the electrostatic interaction existing in a molecule [42–45] is utilized to study the mode of interactions between the fatty acid and tripeptides. MEP is an indicator of the charge distribution in a molecule wherein the regions with higher negative potential V(r) values is richer in electron density [46]. Thus, in order to obtain the detailed information of the electrostatic potential distribution in AFA, AVA and its fatty acid complexes, we have mapped the electrostatic potential at B3LYP/6-311G** level of theory on the molecular surface having an isodensity surface value of 0.01a.u as shown in Fig. 8. It is clear from the MEP of AVA-M that the mode of interaction between AVA and fatty acid is very weak such that the Valine residue does not interact with the incoming fatty acid other than just allowing it to pass by. This is however similar to the ONIOM result wherein we found that the residues moved away from the incoming fatty acid during optimization. In the case of AFA-M(C), the higher negative potential prevailing between the phenyl ring and fatty acid molecule is noticed form the MEP map. Thus, there exists larger electron density in that region confirming the presence of electrostatic interaction. Also, as already mentioned earlier sharing of the π clouds of aromatic ring do take place with hydroxyl hydrogen of carboxylic acid present in the fatty acid. This weak interaction is almost sufficient to hamper the passage of fatty acid inside the channel and also to hinder further docking of similar fatty acids leading to the lack of catalytic and hemolytic activities.

Conclusions

A theoretical study on the interaction of myristic fatty acid (M) with the helix of protein Acutohaemolysin and Piratoxin II has been performed using the two layered ONIOM (B3LYP/6-31G*: UFF) method. The results confirm that the mutation of Phenylalanine for Valine residue in Acutohaemolysin hampers the passage of the fatty acid through the channel due to the interaction of the phenyl ring with the carboxylic group of fatty acid. The quantum chemical calculations on the two palindromic tripeptides AVA and AFA and their fatty acid interacted complexes (AVA-M, AFA-M(C) and AFA-M(E)) were also performed at B3LYP/6-311G** level of theory. The interaction of the myristic fatty acid with the two tripeptides is found to be electrostatic and is comparatively larger for AFA. This electrostatic interaction of AFA is sufficient to prohibit the fatty acid from passing into the protein channel, which in turn is found to be possible only when the fatty acid interacts at the center of the phenyl ring of Phenylalanine residue than at the edges. The conformational variation of Phenylalanine in AFA tripeptide after interacting with the fatty acid further elucidates the stronger interaction. The molecular electrostatic potential depicts the π interaction prevailing between the aromatic ring of Phenylalanine and the hydroxyl hydrogen of the fatty acid. Overall this theoretical investigation may aid experimentalists to search further for the toxic/pharmacological effects of these PLA2 proteins.

Acknowledgments A.A is thankful to Council for Scientific and Industrial Research (CSIR) New Delhi for the award of Senior Research Fellowship. Authors are thankful to the National facility established by DST, Government of India, at the Center for Modeling, Simulation and Design (CMSD), Hyderabad for providing the high performance computing facility (HPCF) at which most of the calculations were performed.

References

1. Valentin E, Lambeau G (2000) Increasing molecular diversity of secreted phospholipases A2 and their receptors and binding proteins. Biochim Biophys Acta 1488:59–70
2. Schaloske RH, Dennis EA (2006) The phospholipase A2 superfamily and its group numbering system. Biochim Biophys Acta 1761:1246–1259
3. Kini RM (2003) Excitement ahead: structure, function and mechanism of snake venom phospholipase A2 enzymes. Toxicon 42:827–840
4. Doley R, Mukherjee AK (2003) Purification and characterization of an anticoagulant phospholipase A2 from Indian monocled cobra (Naja kaouthia) venom. Toxicon 41:81–91
5. Doley R, King GF, Mukherjee AK (2004) Differential hydrolysis of erythrocyte and mitochondrial membrane phospholipids by two phospholipase A2 isoenzymes (NK-PLA2-I and NK-PLA2-II), from Indian monocled cobra Naja kaouthia venom. Arch Biochem Biophys 425:1–13
6. Mukherjee AK (2007) Correlation between the phospholipids domains of the target cell membrane and the extent of Naja kaouthia PLA2-induced membrane damage: evidence of distinct catalytic and cytotoxic sites in PLA2 molecules. Biochim Biophys Acta 1770:187–195

7. Chang CC (1985) Neurotoxins with phospholipase A2 activity in snake venoms. Proc Natl Sci Council B ROC 9:126–142
8. Gutiérrez JM, Lomonte B (1997) Phospholipase A2 myotoxins from Bothrops snake venoms. In: Kini RM (ed) Venom phospholipase A2 enzymes: structure, Function and mechanism. Wiley, Chichester, England, pp 321–352
9. Berg OG, Gelb MH, Tsai MD, Jain MK (2001) Interfacial enzymology: the secreted phospholipase A2-paradigm. Chem Rev 101:2613–2654
10. Gutiérrez JM, Ownby CL (2003) Skeletal muscle degeneration induced by venom phospholipases A2: insights into the mechanisms of local and systemic myotoxicity. Toxicon 42:915–931
11. Ponce-Soto LA, Bonfim VL, Rodrigues-Simioni L, Novello JC, Marangoni S (2006) Determination of primary structure of two isoforms 6-1 and 6-2 PLA2 D49 from Bothrops jararacussu snake venom and neurotoxic characterization using in vitro neuromuscular preparation. Protein J 25:147–155
12. Gutiérrez JM, Ponce-Soto LA, Marangoni S, Lomonte B (2008) Systemic and local myotoxicity induced by snake venom group II phospholipases A2: comparison between crotoxin, crotoxin B and a Lys49 PLA2 homologue. Toxicon 51:80–92
13. Diaz C, Gutiérrez JM, Lomonte B (1992) Isolation and characterization of basic myotoxic phospholipases A2 from Bothrops godmani (Godman's pit viper) snake venom. Arch Biochem Biophys 298:135–142
14. Chaves F, León G, Alvarado VH, Gutiérrez JM (1998) Pharmacological modulation of edema induced by Lys-49 and Asp-49 myotoxic phospholipases A2 isolated from the venom of the snake Bothrops asper (terciopelo). Toxicon 36:1861–1869
15. Landucci ECT, de Castro RC, Pereira MF, Cintra ACO, Giglio JR, Marangoni S, Oliveira B, Cirino G, Antunes E, de Nucci G (1998) Mast cell degranulation induced by two phospholipase A2 homologues: dissociation between enzymatic and biological activities. Eur J Pharmacol 343:257–263
16. Andriáo-Escarso SH, Soares AM, Rodrigues VM, Aˆngulo Y, Diaz C, Lomonte B, Gutierrez JM, Giglio JR (2000) Myotoxic phospholipases A2 in Bothrops snake venoms: effect of chemical modifications on the enzymatic and pharmacological properties of bothropstoxins from Bothrops jararacussu. Biochimie 82:755–763
17. Kanashiro MM, Escocard RCM, Petretski JH, Prates MV, Alves EW, Machado OLT, Dias da Silva W, Kipnis TL (2002) Biochemical and biological properties of phospholipases A2 from Bothrops atrox snake venom. Biochem Pharmacol 64:1179–1186
18. Liu Q, Huang Q, Teng M, Weeks CM, Jelsch C, Zhang R, Niu L (2003) The Crystal Structure of a Novel, Inactive, Lysine 49 PLA2 from Agkistrodon acutus Venom. An ultrahigh resolution, ab initio structure determination. J Biol Chem 278:41400–41408
19. Lee WH, Da Silva Giotto MT, Marangoni S, Toyama MH, Polikarpov I, Garratt RC (2001) Structural basis for bow catalytic activity in Lys49 phospholipases A2-A hypothesis: the crystal structure of piratoxin II complexed to fatty acid. Biochemistry 40:28–36
20. Wieczorek R, Dannenberg JJ (2008) Amide I vibrational frequencies of α-helical peptides based upon ONIOM and Density Functional Theory (DFT) studies. J Phys Chem B 112:1320–1328
21. Gherman BF, Goldberg SD, Cornish VW, Friesner RA. Mixed Quantum Mechanical/Molecular Mechanical (QM/MM) study of the deacylation reaction in a Penicillin Binding Protein (PBP) versus in a class C β-lactamase. J Am Chem Soc 126:7652-7664
22. Matsubara T, Dupuis M, Aida M (2007) An insight into the environmental effects of the pocket of the active site of the enzyme. *Ab initio* ONIOM-molecular dynamics (MD) study on cytosine deaminase. J Comput Chem 29:458–465
23. Becke ADJ (1993) Density-functional thermochemistry. III. The role of exact exchange. J Chem Phys 98:5648–5652
24. Lee C, Yang W, Parr RG (1988) Development of the Colle-Salvetti correlation-energy formula into a functional of the electron density. Phys Rev B 37:785–789
25. Ramachandran GN, Sassiekharan V (1968) Conformation of polypeptides and proteins. Adv Prot Chem 28:283–437
26. Mennucci B, Tomasi J (1997) Continuum solvation models: a new approach to the problem of solute's charge distribution and cavity boundaries. J Chem Phys 106:5151–5158
27. Mennucci B, Cancès E, Tomasi J (1997) Evaluation of solvent effects in isotropic and anisotropic dielectrics and in ionic solvents with a unified integral equation method: theoretical bases, computational implementation and numerical applications. J Phys Chem B 101:10506–10517
28. Cammi R, Mennucci B, Tomasi J (1999) Second order Moller-Plesset analytical derivatives for the polarizable continuum method using the relaxed density approach. J Phys Chem A 103:9100–9108
29. Cammi R, Mennucci B, Tomasi J (2000) Fast evaluation of geometries and properties of excited molecules in solution: a Tamm Dancoff model with application to 4-dimethyl aminobenzonitrile. J Phys Chem A 104:5631–5637
30. Murray JS, Politzer P (1998) The molecular electrostatic potential: a tool for understanding and predicting molecular interactions. In: Sapse AM (ed) Molecular orbital calculations for biological systems. Oxford University Press, NY, p 49
31. Náray-Szabó G (1998) Electrostatic catalysis. In: PvR S, Allinger NL, Clark T, Gasteiger J, Kollman PA, Schaefer HF, Schreiner PR (eds) The encyclopedia of computational chemistry. Wiley, Chichester, UK, p 905
32. Köster AM, Leboeuf M, Salahub DR (1996) Molecular electrostatic potentials from density functional theory. In: Murray JS, Sen K (eds) Molecular electrostatic potentials. Concepts and applications. Elsevier, Amsterdam, pp 105–142
33. Koritsánszky TS, Coppens P (2001) Chemical applications of X-ray charge density analysis. Chem Rev 101:1583–1628
34. Frisch MJ, Trucos GW, Schlegel HB, Scuseria GE, Robb MA, Cheeseman JR, Montgomery JA, Vreven JrT, Kudin KN, Burant JC, Millam JM, Iyengar SS, Tomasi J, Barone V, Mennucci B, Cossi M, Scalmani G, Rega N, Petersson GA, Nakatsuji H, Hada M, Ehara M, Toyota K, Fukuda R, Hasegawa J, Ishida M, Nakajima T, Honda Y, Kitao O, Nakai H, Klene M, Li X, Knox JE, Hratchian HP, Cross JB, Adamo C, Jaramillo J, Gomperts R, Stratmann RE, Yazyev O, Austin AJ, Cammi R, Pomelli C, Ochterski JW, Ayala PY, Morokuma K, Voth GA, Salvador P, Dannenberg JJ, Zakrzewski VG, Dapprich S, Daniela AD, Strain MC, Farkas O, Malick DK, Rabuck AD, Raghavachari K, Foresman JB, Ortiz JV, Cui Q, Baboul AG, Clifford S, Cioslowski J, Stefanov BB, Liu G, Liashenko A, Piskorz P, Komaromi I, Martin RL, Fox DJ, Keith T, Al-Laham MA, Peng CY, Nanayakkara A, Challacombe M, Gill PMW, Jonson B, Chen W, Wong MW, Gonzalez C, Pople JA (2003) Gaussian 03, Revision A.1. Gaussian Inc, Pittsburgh, PA
35. Laaksonen L (1992) A graphics program for the analysis and display of molecular dynamics trajectories. J Mol Graph 10:33–34
36. Hummer G, Pratt LR, García AE (1996) Free energy of ionic hydration. J Phys Chem 100:1206–1215
37. Karplus M, Petsko GA (1990) Molecular dynamics simulations in biology. Nature 347:631–639
38. Dokholyan NV, Buldyrev SV, Stanley HE, Shakhnovich EI (2000) Identifying the protein folding nucleus using molecular dynamics. J Mol Biol 296:1183–1188
39. Hassan SA, Mehler EL, Zhang D, Weinstein H (2003) Molecular dynamics simulations of peptides and proteins with a continuum electrostatic model based on screened Coulomb potentials. Proteins 51:109–125
40. Baldoni HA, Rodriguez AM, Zamarbide G, Enriz RD, Farkas O, Csaszar P, Torday LL, Sosa CP, Jalki I, Perczel A, Hollosi M,

Csizmadia IG (1999) An ab initio study on N-formyl-L-prolinamide with trans peptide bond. The existence or non-existence of alpha(L) and epsilon(L) conformations. J Mol Struct THEOCHEM 465:79–91
41. Csaszar AG, Perczel A (1999) Ab initio characterization of building units in peptides and proteins. Prog Biophys Mol Biol 77:243–309
42. Espinosa E, Lecomte C, Ghermani NE, Devémy J, Rohmer MM, Bérnard M, Molins E (1996) Hydrogen bonds: first quantitative agreement between electrostatic potential calculations from experimental X-(X+N) and theoretical ab initio SCF models. J Am Chem Soc 118:2501–2502
43. Galabov B, Bobadova-Parvanova P (2000) Molecular electrostatic potential as reactivity index in hydrogen bond formation: an HF/6–31+G(d) study of hydrogen-bonded (HCN)n clusters, n=2, 3, 4, 5, 6, 7. J Mol Struct 550:93–98
44. Politzer P, Truhlar DG (1981) Chemical applications of atomic and molecular electrostatic potentials. Plenum Press, New York, pp 7–28
45. Chana A, Miguel A, Concejero M, de Frutos G, MJ HB (2002) Computational studies on biphenyl derivatives. Analysis of the conformational mobility, molecular electrostatic potential, and dipole moment of chlorinated biphenyl: searching for the rationalization of the selective toxicity of Polychlorinated Biphenyls (PCBs). Chem Res Toxicol 15:1514–1526
46. Poland A, Knutson JC (1982) 2, 3, 7, 8-Tetrachlorodibenzo-thorn-dioxin and related halogenated aromatic hydrocarbons: examination of the mechanism of toxicity. Annu Rev Pharmacol Toxicol 22:517–554